The NHERF2 sequence adjacent and upstream of the ERM-binding domain affects NHERF2–ezrin binding and dexamethasone stimulated NHE3 activity

Jianbo Yang*[1], Rafiquel Sarker*[1], Varsha Singh*, Prateeti Sarker*, Jianyi Yin*, Tian-E Chen*, Raghothama Chaerkady†, Xuhang Li*, C. Ming Tse* and Mark Donowitz*‡[2]

*Departments of Medicine, Division of Gastroenterology, The Johns Hopkins University School of Medicine, Baltimore, Maryland 21205, U.S.A.
†Department of Biological Chemistry, The Johns Hopkins University School of Medicine, Baltimore, Maryland 21205, U.S.A.
‡Department of Physiology, The Johns Hopkins University School of Medicine, Baltimore, Maryland 21205, U.S.A.

In the brush border of intestinal and kidney epithelial cells, scaffolding proteins ezrin, Na^+-H^+ exchanger regulatory factor (NHERF)1 and NHERF2 play important roles in linking transmembrane proteins to the cytoskeleton and assembling signalling regulatory complexes. The last 30 carboxyl residues of NHERF1 and NHERF2 form the EBDs [ezrin, radixin and moesin (ERM)-binding domain]. The current study found that NHERF1/2 contain an ERM-binding regulatory sequence (EBRS), which facilitates the interaction between the EBD and ezrin. The EBRSs are located within 24 and 19 residues immediately upstream of EBDs for NHERF1 and NHERF2 respectively. In OK (opossum kidney) epithelial cells, EBRSs are necessary along with the EBD to distribute NHERF1 and NHERF2 exclusively to the apical domain. Furthermore, phosphorylation of Ser^{303} located in the EBRS of NHERF2, decreases the binding affinity for ezrin, dislocates apical NHERF2 into the cytosol and increases the NHERF2 microvillar mobility rate. Moreover, increased phosphorylation of Ser^{303} was functionally significant preventing acute stimulation of NHE3 (Na^+-H^+ exchanger 3) activity by dexamethasone.

Key words: epithelial cell, ezrin, radixin and moesin-binding regulatory sequence (EBRS), NHE3, microvillus, Na^+-H^+ exchanger regulatory factor (NHERF)1/2, phosphorylation.

INTRODUCTION

The microvillus of epithelial cells is a defining cytoskeletal structure, especially for intestine and kidney [1]. Many of the transporters responsible for nutrition and electrolyte absorption and secretion are distributed in the microvillus. Scaffolding proteins, such as ezrin, Na^+-H^+ exchanger regulatory factor (NHERF)1 and NHERF2, play critical roles not only in anchoring or retaining transporters, receptors and signalling molecules in the microvilli, but also in regulating their functions by assembling them into macro-complexes through multiple protein–protein interaction domains [2–5].

Ezrin is a member of the ERM (ezrin, radixin and moesin) protein family and has an N-terminal FERM (band four-point-one, ERM homology domain) and a C-ERMAD (C-terminal ERM-association domain) [2]. The FERM domain uses several different sites to interact with PIP2 (phosphatidylinositol 4,5-bisphosphate) [6], multiple transmembrane proteins such as NHE3 (Na^+-H^+ exchanger 3) [7], NHE1 [8], ICAM-1 (Intercellular Adhesion Molecule 1), ICAM-2, CD43 (cluster of differentiation 43) and CD44 [2] and other proteins [9]. The C-ERMAD domain either interacts with FERM domain to keep ezrin in a dormant conformation [10] or interacts with F-actin filaments through an actin-binding motif to link activated ezrin to the cytoskeleton [11]. NHERF1 and NHERF2 belong to the NHERF family of proteins, which contains multiple PDZ [postsynaptic density 95/discs large/zona occludens-1 (ZO-1)] domains [3].

NHERF1 and NHERF2 are two closely related homologues containing two N-terminal PDZ domains, a C-terminal EBD (ERM-binding domain) and non-conserved linkers [3,12]. The PDZ domains are able to interact with multiple PDZ-recognition motif containing proteins including NHE3, CFTR (cystic fibrosis transmembrane conductance regulator), DRA (down-regulated in adenoma), Na/Pi-II (sodium-dependent phosphate transporter), multiple other transporters, as well as G protein-coupled receptors and cytosolic signalling effector proteins [3,4,13]. The EBD interacts with FERM domain of ezrin leading to indirect attachment to the cytoskeleton [14,15]. Recently, we reported that the non-conserved region upstream of the EBD was involved in the association of NHERF2 with the cytoskeleton, although the detailed mechanism remained unknown [12].

Ezrin, NHERF1 and NHERF2 all directly interact with NHE3 and contribute to the microvillar immobilization of NHE3 [7,16,17]. NHE3 is mainly expressed in the kidney and intestine and contributes to sodium absorption [3,7,16–18]. Ezrin, NHERF1 and NHERF2 also play important roles in the organization of signalling complexes through which multiple aspects of regulation of NHE3 occur [17,19–22]. Understanding the roles of NHERF proteins in the regulation of NHE3 should help to develop better strategies to stimulate intestinal NHE3 activity, which is inhibited in diarrhoeal diseases [19,20].

Although the epithelial cell microvillus scaffolding proteins have been generally thought to form a stable structure related to the presence of a large cytoskeletal component, we and others demonstrated that NHERF1 and NHERF2 are surprisingly mobile in the microvilli of several cell lines including OK (opossum kidney proximal tubule cell), Caco-2 (human epithelial colorectal adenocarcinoma cell) and JEG-3 (human placental

choriocarcinoma cell) [5,12,23]. Other microvilli resident components including F-actin, ezrin and MYO1A (Myosin-Ia) have also been shown to be highly dynamic and mobile [24–26]. As summarized by a recent review [5], this is also true for other scaffolding proteins, including Ste5p localized to the tips of mating projections in budding yeast, E-cadherin–β-catenin–α-catenin complex localized at cell–cell adhesions, ZO-1 localized at the cell tight junctions and multiple synaptic scaffolding proteins, SAP102 (synapse-associated protein 102), SAP-97 and PSD-95 (postsynaptic density 95) [27]. Most of these studies have attributed the mobile nature of scaffolding proteins to their intrinsic dynamic association and dissociation with their binding partners in these 'stable' cellular complexes.

The critical partners have not been characterized that determine the microvillar mobility of NHERF1 and NHERF2. As the major ERM protein expressed in epithelial cells, ezrin could be the critical binding partner since EBDs are necessary for the localization of NHERF1/2 to the microvillus [14,15,22,28–30]. However, the slower mobility rate and tighter cytoskeleton association of NHERF2 compared with NHERF1 [12,23], could not be accounted for just by their EBDs, since the NHERF2–EBD has a lower binding affinity than NHERF1–EBD for radixin, a homologue of ezrin [29]. Confusingly, two recent studies reported that full-length NHERF2 co-immunoprecipitated more ezrin than did full-length NHERF1 [23,31]. These apparently contradictory results could be resolved if any other elements of NHERF1 and NHERF2 were somehow involved in ezrin binding. In fact, it was demonstrated that the slower mobility of NHERF2 is determined by a unique C-terminal domain, which includes not only the EBD but also its upstream non-conserved region [12]. This led us to hypothesize that the non-conserved region upstream of the EBD modulates the interaction between the EBD and ezrin in NHERF2, therefore contributing to determine the ezrin-binding affinity and the microvillar mobility of NHERF2.

EXPERIMENTAL

Materials, plasmids and antibodies

GSH-resin (glutathione sepharose 4B resin) was from GE Healthcare Life Science. Amylose resin and rabbit anti-MBP (Maltose-Binding Protein) were from NEB (New England Biolabs). Ni-NTA (nitrilotriacetic acid) resin was from Qiagen. BCECF-AM (2′,7′-Bis-[2-Carboxyethyl]-5-[and-6]-Carboxyfluorescein, Acetoxymethyl Ester), nigericin, Hoechst 33342 and tetramethyl-rhodamine-conjugated WGA (wheat germ agglutinin) were from Life Technologies. Glutathione, maltose, mouse anti-FLAG, anti-FLAG M2 magnetic beads, mouse anti-His$_6$, rabbit anti-NHERF1 and rabbit anti-NHERF2 were from Sigma. Mouse anti-VSV-G (vesicular stomatitis virus envelope glycoprotein) was produced from hybridoma P5D4 clone. Mouse anti-GST was from Cell Signaling Technology. IRdye-700 or IRdye-800 conjugated goat anti-mouse or goat anti-rabbit secondary antibodies were from Rockland Immunochemicals Inc. and were used with the LI-COR Odyssey system for Western blot analysis.

Plasmid pCB6-N-ezrin encoding VSV-G tagged N-terminal ezrin [1–309 amino acids (aa)] was a gift from Dr Monique Arpin [32]. Plasmids pFLAG–NHERF1/2/3 and pmEOS2–NHERF1/2 were constructed previously [12,33]. Fluorescent protein mEOS2 was fused to a FLAG-tag in p3XFLAG–CMV-10 (Sigma) to construct pFLAG–mEOS2, which was used to make constructs expressing FLAG–mEOS2-fused NHERF1 C-termini C30 and C54 and NHERF2 C-termini C30 and C49 (Figure 1). All the fusion tags were at the N-terminus of NHERF proteins or

fragments. NHERF2 mutants S303A, S303D, T305A, T305D and T305E were generated by QuickChange II Site-Directed Mutagenesis Kits (Agilent Technologies).

Cell culture

OK proximal tubular cells and HEK-293A cells were transfected at 90 % confluency with Lipofectamine 2000 (Life Technologies) for co-immunoprecipitation (IP) or pull-down studies 48 h later. The human colon cancer Caco-2/bbe cell line grown on collagen coated Transwell filter membranes (EMD Millipore) was infected with Adeno–FLAG–NHERF2 virus as described previously [21] for IP of FLAG–NHERF2 48 h later and was used for MS analysis.

Immunoprecipitation

Cell lysate was prepared with lysis buffer (25 mM HEPES, pH 7.4, 150 mM NaCl, 50 mM NaF, 1 mM Na$_3$VO$_4$, 0.5 % Triton X-100 and protease inhibitors). For experiments in Figure 2, 1 mg of cell lysate was mixed with 10 μl of pre-washed anti-FLAG M2 magnetic beads and incubated at 4°C for 3 h on a rotating shaker. For experiments in Figures 7 and 9, 1.5 mg of cell lysate and 20 μl of anti-FLAG M2 magnetic beads were used and overnight incubations were performed. Beads were washed with the same lysis buffer four times and eluted with 1.5× Laemmli sample buffer without 2-mercaptoethanol. Samples were analysed by Western blot. For MS studies in Figure 7, FLAG–NHERF2 was eluted from beads with 100 mM glycine/HCl, pH 3.0, and adjusted to pH 7.0 with 0.5 M HEPES buffer pH 7.4.

Recombinant protein purification

MBP–NHERF1/2 and GST-N–ezrin (GST-tagged N-terminal ezrin 1–309 aa) were purified as previously described [7,33]. DNAs encoding the C-terminal fragments of NHERF1 and NHERF2 were generated by PCR and inserted into pET32a (EMD Millipore) for expressing both His$_6$ and thioredoxin (His$_6$–thioredoxin) fused recombinant proteins (Figure 1). These constructs were transformed into BL21(DE3) strain (EMD Millipore) for IPTG-induced protein expression. Proteins were purified with Ni-NTA resin following the manufacturer's instructions. Purified proteins were supplemented with 10 % glycerol and 10 mM DTT and stored at − 80°C.

GSH–resin pull-down

For Figures 2–5 and 8, 1 nmol of recombinant GST-N–ezrin was used as bait for pull-downs. For binary interaction studies, 3 nmol of purified proteins were used as prey. For competition experiments between two NHERF fragments or full-length proteins, 3 nmol of each purified protein were used. For competition experiments described in Figure 4, 1 nmol of GST-N–ezrin was first pre-incubated with 3 nmol of His$_6$–thioredoxin or His$_6$–thioredoxin fused NHERF C-terminus fragments for 30 min, then 1 mg of Caco-2 cell lysate was added. The volume of final mixture was adjusted to 500 μl. Each bait–prey mixture was mixed with 10 μl of pre-washed GSH-resin and incubated at 4°C for 3 h on a rotating shaker. Resin was washed four times and eluted with lysis buffer plus 10 mM glutathione. For Figure 9, 3 μg of purified GST-N–ezrin was mixed with 1.5 mg of HEK-293A cell lysate expressing FLAG–NHERF2 or mutants and 10 μl of GSH–resin for overnight incubation at 4°C. Resin was washed four times and finally eluted with 2× Laemmli buffer at 80°C.
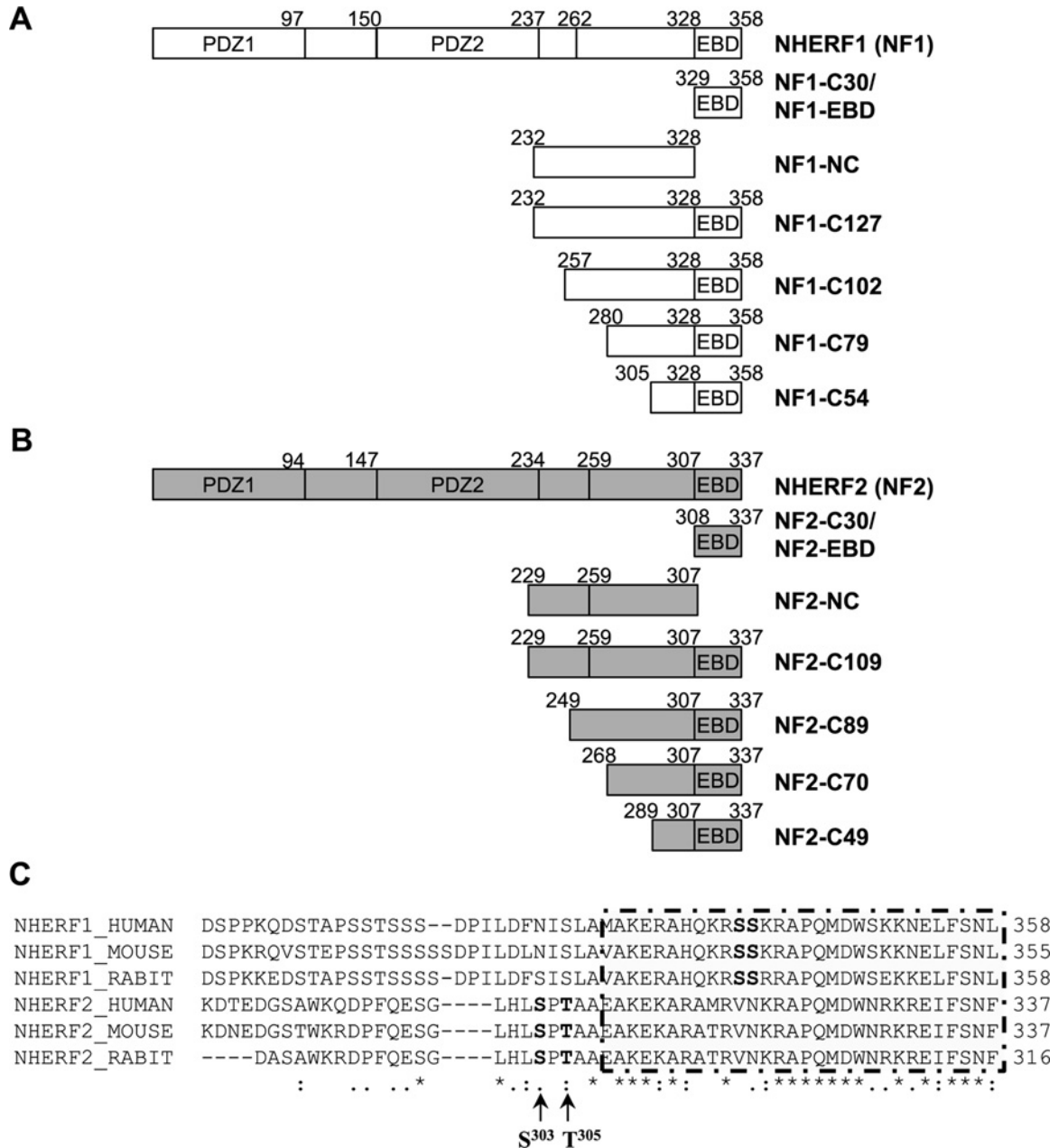
Figure 1   Diagram of full-length NHERF1, NHERF2 and their C-terminal fragments used in the present study

All the tags, including FLAG, MBP, His$_6$–thioredoxin (His$_6$ and thioredoxin) and FLAG–mEOS2, were fused to the N-terminus of NHERF proteins or fragments. (**A**) FLAG, MBP, His$_6$–thioredoxin or mEOS2-fused full-length NHERF1 (NF1) or NHERF1 C-terminal fragments C127, NC, C30, C102, C79 and C54 were used in later studies. (**B**) FLAG, MBP, His$_6$–thioredoxin or mEOS2-fused full-length NHERF2 (NF2) or NHERF2 C-terminal fragments C109, NC, C30, C89, C70 and C49 were used in later studies. (**C**) Protein sequences of NHERF1 and NHERF2 from *Homo sapiens*, *Mus musculus* and *Oryctolagus cuniculus* were aligned with Clustal W software. EBD is framed by dash-dot lines. NHERF2 Ser^{303} and Thr^{305} were shown to be phosphorylated in the present study. The two NHERF1 serine residues in bold were previously reported to be phosphorylated [37].

LC–MS/MS

Samples were proteolysed using the 'Filter Assisted Sample Preparation' (FASP) method [34]. Briefly, samples were reduced with 5 mM TCEP (tris[2-carboxyethyl]phosphine) at 37 °C for 45 min and reduced cysteines were blocked using 10 mM iodoacetamide at 25 °C for 15 min. Samples were then cleaned using 30 kDa Amicon Filter (EMD Millipore) three times using 9 M urea and two times using 50 mM triethyl ammonium bicarbonate. Samples were then proteolysed with trypsin/lysC

(Promega) for 12 h at 37 °C. Peptide samples were desalted using stage-tip C18 (3M Emphore).

Protein identification by LC–MS/MS analysis of peptides was performed on a Q-Exactive instrument (Thermo Fisher Scientific) interfaced with the Proxion nanoflow LC system. Peptides were separated on a reversed-phase HPLC on a 75 μm × 15 cm PicoFrit column (New Objective) packed with Magic C18AQ [5 μm, 120 Å (1 Å = 0.1 nm), Michrom Bioresources]. Peptides were separated using a gradient of 0 %–60 % acetonitrile/0.1 % formic acid over 70 min at a flow rate of 300 nl/min. Eluting
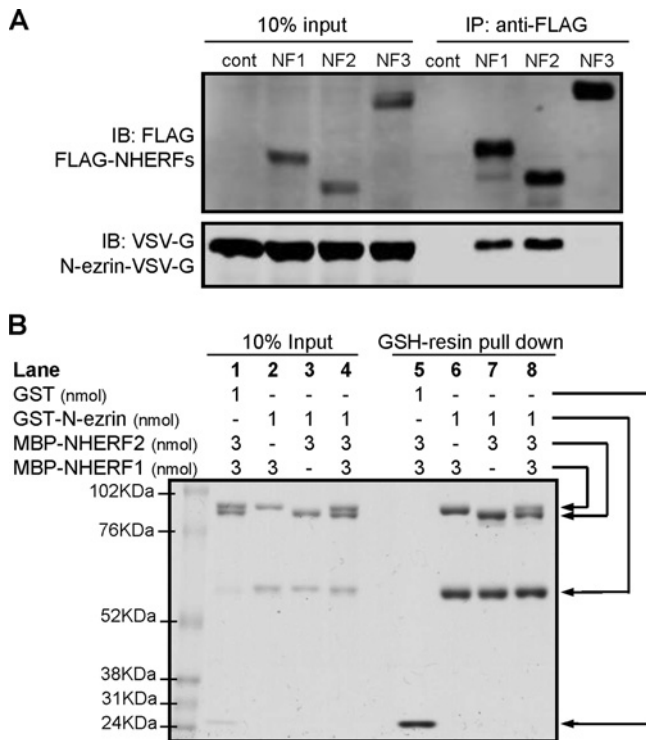
A

IB: FLAG
FLAG-NHERFs

IB: VSV-G
N-ezrin-VSV-G

B

Figure 2   Full-length NHERF2 has higher binding affinity for ezrin than full-length NHERF1

(**A**) OK cells were co-transfected with pCB6-N–ezrin and pFLAG–NHERFs (NF1, NF2 or NF3) and then subjected to IP with anti-FLAG magnetic beads. Empty vector was used as control (cont). Samples were analysed by Western blot with antibodies against VSV-G and FLAG. (**B**) In 500 μl of buffer, 1 nmol of GST or GST-N–ezrin protein was mixed with 3 nmol of MBP–NHERF1 or MBP–NHERF2 or both and then subjected to pull-down with GSH–resin. GST was used in lane 1 as a negative control. The label '-' was used to indicate that protein was not used (same for all the following figures). Samples were analysed by Coomassie Blue staining. Experiments were repeated three times and one representative result is shown.

peptides were sprayed directly into Q-Exactive at 2.0 kV spray voltage. Survey scans were acquired from 350–1800 *m/z* with up to 15 peptide masses (precursor ions) individually isolated with a 2 Da window with 0.5 Da offset and fragmented (MS/MS) using a collision energy of 27 and 30 s dynamic exclusion. Precursor and the fragment ions were analysed at 70000 and 17500 resolution respectively. Peptide sequences were identified from isotopically resolved masses in MS and MS/MS spectra extracted with and without deconvolution using Thermo Scientific MS2 processor and Xtract software. Data was searched against human 2012, database with oxidation on methionine, deamidation on residues asparagine and glutamine, phospho S/T/Y, (as different variable modifications) and carbamidomethyl on cysteine, as fixed modifications using Mascot software interfaced with the Proteome Discoverer 1.4 (http://portal.thermo-brims.com/) workflow. Peptide identifications from Mascot searches were processed within Proteome Discoverer software to identify peptides with a confidence threshold < 1% false discovery rate, based on a concatenated decoy database search to calculate the median protein and peptide ratios. Localization of phosphotyrosine sites was evaluated using PhosphoRS score and manual inspection.

Confocal imaging analysis of NHERF distribution

OK cells were grown in glass-bottom dishes and transiently co-transfected with pmEOS2–NHERF or pFLAG–mEOS2-NHERF

constructs as indicated on the second day post confluency and used 48 h later. For live cell imaging, cells were incubated with Hoechst 33342 for 30 min at 37 °C and then washed with no Phenol Red medium. Dishes were mounted on a Zeiss LSM 510 confocal microscope equipped with a climate controlled chamber to image the green fluorescence of mEOS2 and the nuclear staining. For co-staining with surface marker WGA, cells were cooled down by washing with ice-cold PBS three times, incubated with tetramethyl–rhodamine–WGA at 4 °C for 1 h, then washed with PBS, fixed with 4% paraformaldehyde and mounted on the microscope for imaging.

NHE3 activity

Na$^+$/H$^+$ exchange activity was determined as previously described [7,22] in OK cells expressing endogenous NHE3 seeded on glass coverslips. At ∼90% confluency, cells were transfected with pcDNA3.1/FLAG–NHERF2–WT (wild-type) or S303A/D mutants and used ∼48 h later. Cells were serum starved overnight and NHE3 activity was determined after 4 h of treatment with 10 μM dexamethasone. Changes in intracellular pH (pH$_i$) were measured fluorometrically using BCECF-AM in a Quantamaster fluorometer from Photon Technology International. The initial rates of Na$^+$-induced recovery of pH$_i$ after an acute acid load caused by prepulsing with NH$_4$Cl were calculated for a given pH$_i$ over the initial 1 min of Na$^+$-dependent intracellular alkalinization and expressed as ΔpH/ΔT. Means $\pm$ S.E.M. were determined from at least three experiments.

FRAP

FRAP was performed on the stage, heated to 37 °C, of a Zeiss LSM 510 confocal microscope equipped with a C-Apochromat 63×/1.2 Korr water-immersion objective, as described previously [12]. OK cells grown in glass-bottom dishes were transiently transfected with pmEOS2–NHERF1, pmEOS2–NHERF2 or NHERF2 mutants and used for FRAP 48 h later. Optical slices were focused on the cell apical domain with a slice thickness of 3 μm. Fluorescence within the ROI (region of interest) was measured at low laser power before the bleach and then photobleached with high laser power. Recovery was followed with low laser power at 5 or 10 s intervals for up to 5 min. The recovery ratios were calculated as the percentage of maximal bleached fluorescence.

RESULTS

Full-length NHERF2 has higher affinity for ezrin than full-length NHERF1

NHERF2 was previously shown to have slower microvillar mobility and tighter association with certain cytoskeleton partners compared with NHERF1 [12]. Ezrin is one of the best characterized cytoskeleton partners for both NHERF1 and NHERF2 [3] and it is more fixed in the microvilli compared with NHERF1 and NHERF2 [5,35]. However, the relative strengths of interactions between ezrin and NHERF1/2 have never been compared. OK cells transiently expressing FLAG-tagged NHERFs and VSV-G fused N-ezrin (N-terminal FERM domain of ezrin) were used for IP with anti-FLAG beads. More N-ezrin was co-immunoprecipitated by FLAG–NHERF2 than that by FLAG–NHERF1 (Figure 2A).

In pull-down assays with purified proteins, when 1 nmol of GST-N–ezrin was mixed with 3 nmol of individual MBP–NHERF1 or MBP–NHERF2, similar amounts of NHERF1

and NHERF2 were pulled-down by GST-N–ezrin (Figure 2B, lanes 6 and 7). As a negative control, GST did not pull-down any detectable NHERF1 and NHERF2 (Figure 2B, Lane 5). Each protein used in this assay was in the micromolar range. It was reported that NHERF1 and NHERF2 interact with the FERM domain of ERM proteins in a 1:1 stoichiometry with the dissociation constant in the nanomolar range [29]. Therefore, it is not surprising that no difference was seen in this assay due to saturated binding. For this reason, in order to identify differences between the binding affinities of NHERF1 and NHERF2, a competitive ezrin-binding assay was designed by mixing 1 nmol of GST-N–ezrin with 3 nmol of MBP–NHERF1 and 3 nmol of MBP–NHERF2. GST-N–ezrin pulled-down more MBP–NHERF2 than MBP–NHERF1 (Figure 2B, Lane 8). Therefore, both co-IP and pull-down methods indicate that full-length NHERF2 has higher affinity for ezrin than full-length NHERF1, perhaps explaining why NHERF2 has a slower microvillar mobility rate [12].

The non-conserved regions upstream of EBDs enhance the interaction between EBD and ezrin for both NHERF1 and NHERF2

In both NHERF1 and NHERF2, the last 30 amino acid residues at the C-terminus form EBDs which interact with ERM proteins with 1:1 stoichiometry [29,30]. By SPR (surface plasmon resonance) analysis, the dissociation constant of EBDs for radixin is 1.7 and 9.5 nM for NHERF1 and NHERF2 respectively [29]. This seemed contradictory to the result above that full-length NHERF2 has higher affinity for ezrin than NHERF1. One possibility is that the binding affinities of EBDs of NHERF1/2 proteins for ezrin are inversely correlated with their affinities for radixin. Another possibility is that the non-conserved regions upstream of EBDs modulate the interaction with ezrin in full-length proteins, since these regions are involved in determining the microvillar mobility of NHERF proteins [12].

To test these possibilities, the C-terminal fragments of NHERF1 and NHERF2 were fused to both His_6 and thioredoxin (His_6–thioredoxin) tags (Figure 1). NHERF1–C30 and NHERF2–C30 contain only the EBD. NHERF1–NC and NHERF2–NC contain the non-conserved linker between PDZ2 and EBD. NHERF1–C127 and NHERF2–C109 contain both EBD and the non-conserved linker. In the binary interaction assays, both NHERF1–C30 and C127 bound to GST-N–ezrin but NHERF1–NC (non-conserved) did not (Figure 3A, left). Similarly, both NHERF2–C30 and C109 bound to GST-N–ezrin but NHERF2–NC did not (Figure 3A, right). In the competitive ezrin-binding assays, NHERF1–C127 outcompeted NHERF1–C30 (Figure 3B, lanes 1 and 7) and NHERF2–C109 outcompeted NHERF2–C30 (Figure 3B, lanes 2 and 8). This suggests that the non-conserved regions upstream of EBDs increase the strength of interaction between EBDs and ezrin in both NHERF1 and NHERF2.

Competition for ezrin binding was also tested between NHERF1–EBD and NHERF2–EBD (Figure 3B, lanes 6 and 12). However, NHERF1–C30 and NHERF2–C30 have approximately the same molecular mass and could not be distinguished by Coomassie staining. Western-blot with anti-NHERF2 antibody was used to distinguish them (Figure 3C). NHERF2 antibody recognizes both NHERF1–C30 and NHERF2–C30 but prefers NHERF2–C30. Western-blot with anti-His_6 was used for normalization, since both NHERF1–C30 and NHERF2–C30 have the same His_6-tag. For each band in lanes 1–4, 6 and 12, the ratio of anti-NHERF2 intensity to anti-His_6 intensity was calculated and plotted (Figure 3C). Lanes 1 and 3 represent such a ratio

for 100% NHERF1–C30 and lanes 2 and 4 represent such a ratio for 100% NHERF2–C30. Lane 6 contains an equimolar mixture of NHERF1–C30 and NHERF2–C30, therefore having an intermediate ratio. The ratio for lane 12 resembles the ratio for 100% NHERF1–C30, indicating that lane 12 contains more NHERF1–C30 than NHERF2–C30 (Figure 3C), suggesting that NHERF1–C30 outcompetes NHERF2–C30. Therefore, the affinities of EBDs of NHERF1/2 for ezrin follow the same trend as their affinities for radixin [29]. In contrast, NHERF2–C109 outcompeted NHERF1–C127 (Figure 3B, lanes 5 and 11), suggesting that the non-conserved region of NHERF2 increases the strength of interaction between EBD and ezrin more than the non-conserved region of NHERF1 does. This may provide the explanation why full-length NHERF2 has a higher affinity for ezrin than full-length NHERF1.

In the competitive ezrin-binding assay, when the amount of GST-N–ezrin and NHERF2–C109 was fixed and the ratio of NHERF1–C127 to NHERF2–C109 was increased between 4:1 and 8:1, NHERF2–C127 and NHERF2–C109 were pulled-down in approximately similar amounts (Figure 4A). It was thus estimated that the ezrin-binding affinity of NHERF2–C109 is ∼4–8-fold higher than that of NHERF1–C127.

GST-N–ezrin pulled-down detectable amounts of endogenous NHERF1 and NHERF2 from Caco-2 lysates (Figure 4B). When GST-N–ezrin was pre-incubated with excessive amounts of NHERF1–C30 and NHERF2–C30, NHERF1 and NHERF2 were pulled-down almost in the same amount. However, constructs containing both EBD and its upstream non-conserved region, NHERF1–C127 and NHERF2–C109 reduced the amount of NHERF1 and NHERF2 that were pulled-down by GST-N–ezrin (Figure 4B). This suggests first that the non-conserved region is required to mimic and fully compete with the full-length NHERF1/2 in ezrin binding; and second that, in full-length NHERF1/2, the non-conserved regions enhance ezrin binding in a way that is similar to what occurs in purified C-terminal fragments.

The adjacent 24 and 19 residues upstream of EBDs are sufficient to enhance ezrin binding for NHERF1 and NHERF2 respectively

To determine the minimal non-conserved sequences required for enhancing ezrin binding, additional NHERF1 and NHERF2 C-terminal fragments were constructed (Figure 1). NHERF1 C-termini C54, C79 and C102 have similar ezrin-binding affinity to NHERF1–C127. All of them outcompeted NHERF1–C30 (Figure 5A). This indicates that the adjacent 24 amino acid residues upstream of EBD in NHERF1–C54 are sufficient to increase the binding between ezrin and NHERF1–EBD. Similarly, NHERF2 C-termini C49, C70 and C89 have similar ezrin-binding affinity to NHERF2–C109. All of them outcompeted NHERF2–C30 (Figure 5B). Therefore, the 19 amino acid residues upstream of EBD are sufficient to enhance the binding between ezrin and NHERF2–EBD.

Although EBDs are necessary for the microvillar localization of NHERF1 and NHERF2 [22,28], it is unknown whether EBDs are sufficient. In live OK cells, mEOS2-fused NHERF1 and NHERF2 were co-localized with the apical surface marker WGA and primarily distributed to microvillar clusters in similar morphology as demonstrated previously by electron microscopy [36] (Figures 6A–6C). As a control, the fusion tag FLAG–mEOS2 was uniformly distributed in the cytosol but not in the clusters of microvilli (Figure 6D). Unlike full-length NHERF1/2, FLAG–mEOS2–NHERF1–C30 and FLAG–mEOS2–NHERF2–C30 had a large cytosolic portion in addition to the microvillar distribution

A. Binary interaction between N-ezrin and NHERF1/2 C-termini
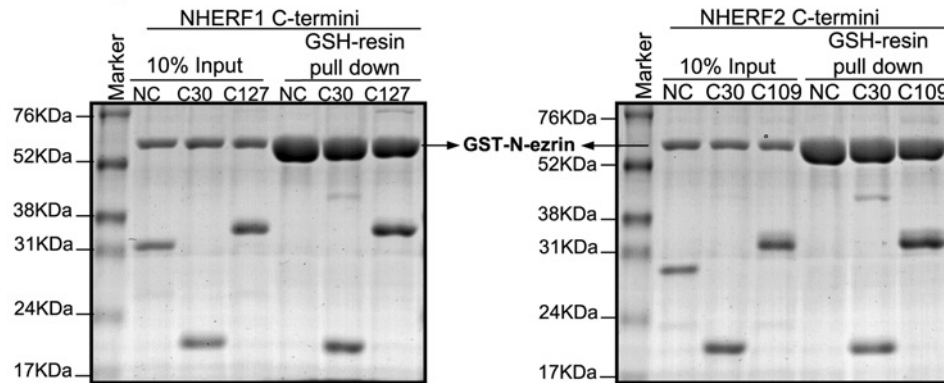
B. Competitive binding for N-ezrin between two of the NHERF1/2 C-termini
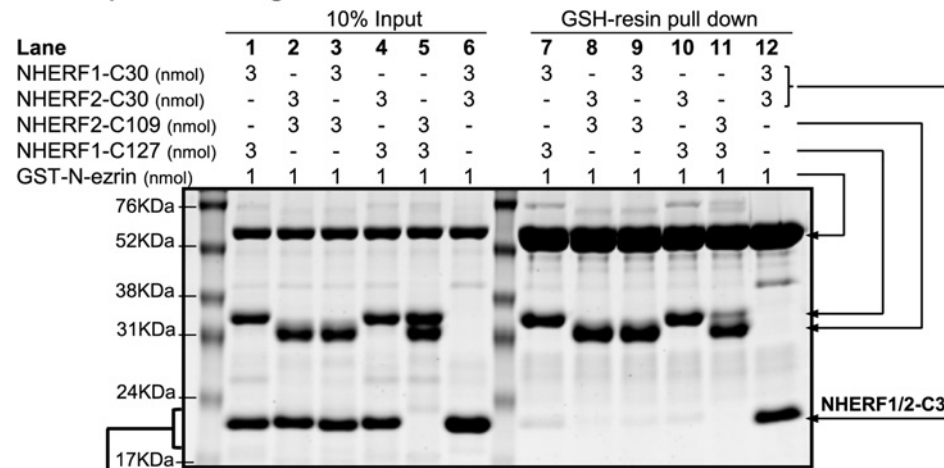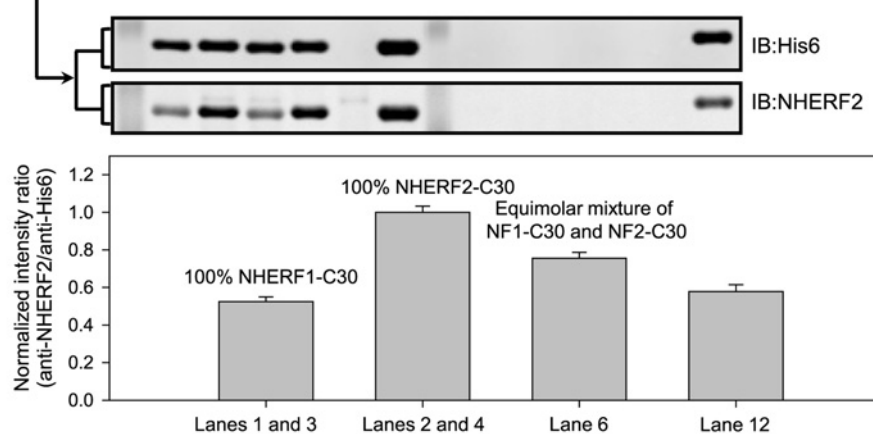

Figure 3   The non-conserved regions upstream of EBDs enhance the interaction between EBD and ezrin for both NHERF1 and NHERF2

(**A**) One nanomole of GST–N–ezrin protein was mixed with 3 nmol of individual His$_6$–thioredoxin fused C-termini from NHERF1 or NHERF2 for GSH-resin pull-down. (**B**) GST–N–ezrin protein was mixed with two of the His$_6$–thioredoxin fused NHERF1/2 C-termini as indicated for pull-down. Both samples in (**A**) and (**B**) were analysed by Coomassie Blue staining. (**C**) Samples in (**B**) were also analysed by Western blot with anti-His$_6$, which is present on both C30 proteins and anti-NHERF2, which has some titre against NHERF1, to determine the relative amounts of NHERF1–C30 and NHERF2–C30 in lane 12. For each band in lanes 1–4, 6 and 12, anti-NHERF2 intensity was divided by anti-His$_6$ intensity to give a normalized ratio, which was plotted. The ratio for NHERF1–C30 alone was derived from the average of lanes 1 and 3; the ratio for NHERF2–C30 alone was derived from the average of lanes 2 and 4; lane 6 contains equimolar ratio of NHERF1–C30 and NHERF2–C30. According to the plot, lane 12 should contain more of NHERF1–C30 than NHERF2–C30. Experiments were repeated three times and one representative result is shown for (**A**) and (**B**). Values presented in (**C**) are means $\pm$ S.D.

(Figures 6E and 6F). However, FLAG–mEOS2–NHERF1–C54 and FLAG–mEOS2–NHERF2–C49 showed similar distribution to full-length NHERF1/2 (Figures 6G and 6H). This kind of difference is not due to different protein expression levels as shown by the Western blot analysis (Figure 6I). Therefore, the

adjacent 24 residues in NHERF1 and 19 residues in NHERF2 upstream of their EBDs were designated as the EBRS (ERM-binding regulatory sequence), since they not only modulate ezrin binding but also are essential for the microvillar distribution of NHERF1/2.
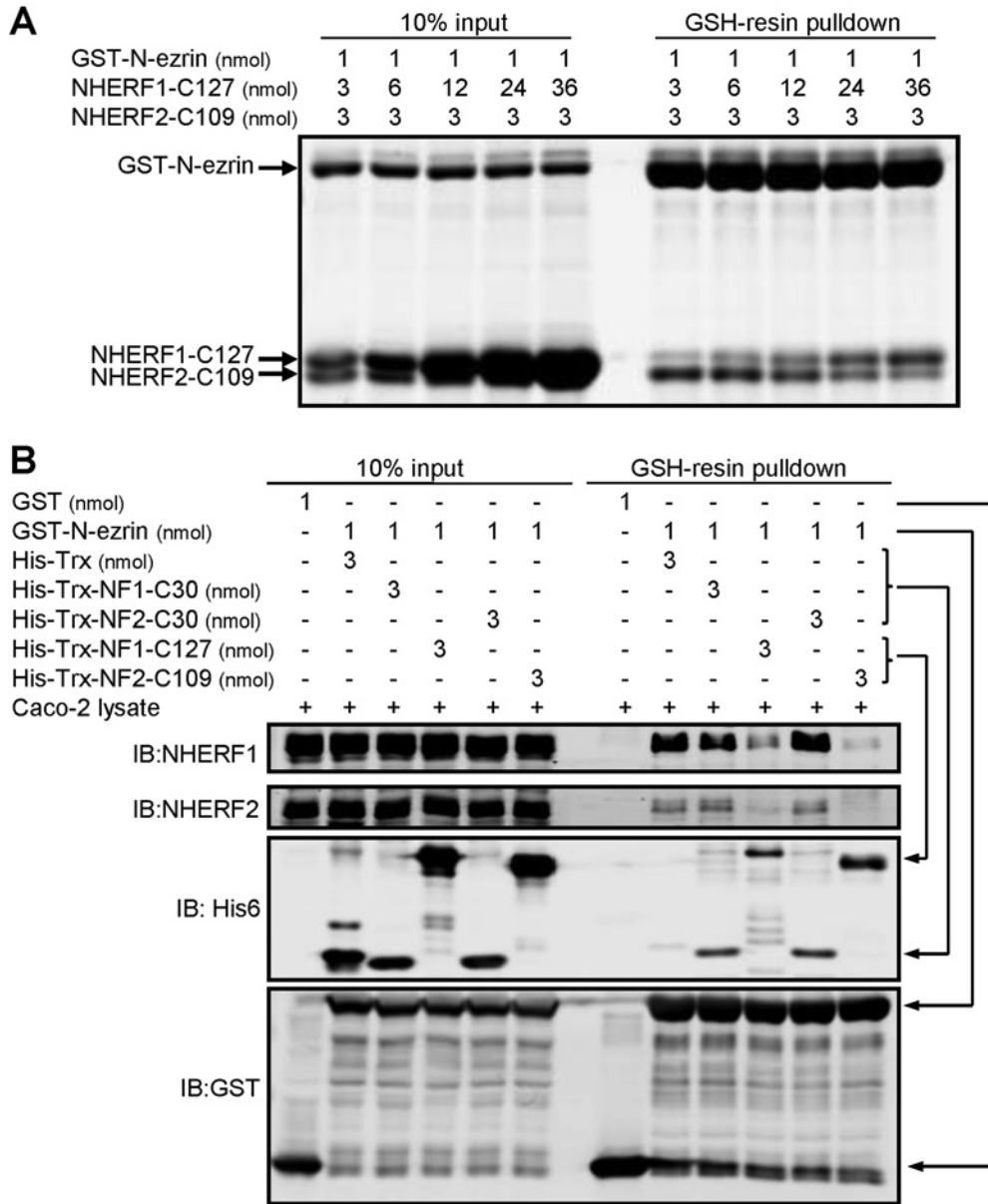
Figure 4   NHERF2–ezrin interaction is stronger than NHERF1–ezrin interaction

(**A**) One nanomole of GST-N–ezrin was mixed with 3 nmol of NHERF2–C109 and varied amounts of NHERF1–C127 as indicated for pull-down. Samples were analysed by Coomassie Blue staining. (**B**) Indicated amounts of GST-N–ezrin protein were pre-incubated with His_6–thioredoxin or His_6–thioredoxin fused NHERF1 or NHERF2 C-termini and then mixed with Caco-2 lysates for pull-down as described in 'Experimental'. Samples were analysed by Western blot. GST was used as negative control and did not pull down NHERF1 or NHERF2. NHERF1–C127 and NHERF2–C109 efficiently competed with full-length NHERF1 and NHERF2, whereas NHERF1–C30 and NHERF2–C30 did not. Experiments were repeated three times and one representative result is shown.

Phosphorylation of Ser[303] located in the EBRS regulates the interaction between NHERF2 and ezrin

The interaction between NHERF1 and ezrin is regulated by phosphorylation sites located inside the EBD [37]. However, no phosphorylation site has been reported in the EBD of NHERF2 according to the PhosphoSitePlus database [38]. MS (mass spec) was used to identify possible NHERF2 phosphorylation sites. FLAG-tagged NHERF2 was transiently expressed in Caco-2/Bbe cells by adenoviral infection and purified by IP. MS analysis of immunoprecipitated FLAG–NHERF2 identified that Ser[303] and Thr[305] were phosphorylated (Figures 7A and 7B) and located within the EBRS of NHERF2 (Figure 1C). No

phosphorylation site was identified in the EBD of NHERF2. Although phosphorylation of Ser[303] has been previously identified in endogenous NHERF2 from mouse and rat tissues [39,40] and human cancer cell lines [41,42], no functional relevance of this phosphorylation has been described. We hypothesized that phosphorylation of Ser[303] or/and Thr[305] might play a role in modulating NHERF2–ezrin binding.

NHERF2 mutants S303A, S303D, T305E and T305A were generated. Binary interaction assays could not detect any difference in ezrin binding among all these mutants (Figure 8A). However, competitive ezrin-binding assays showed that only NHERF2–C49 S303A had the same capability as WT NHERF2–C49 in competition with both NHERF2–C30 (Figure 8B) and
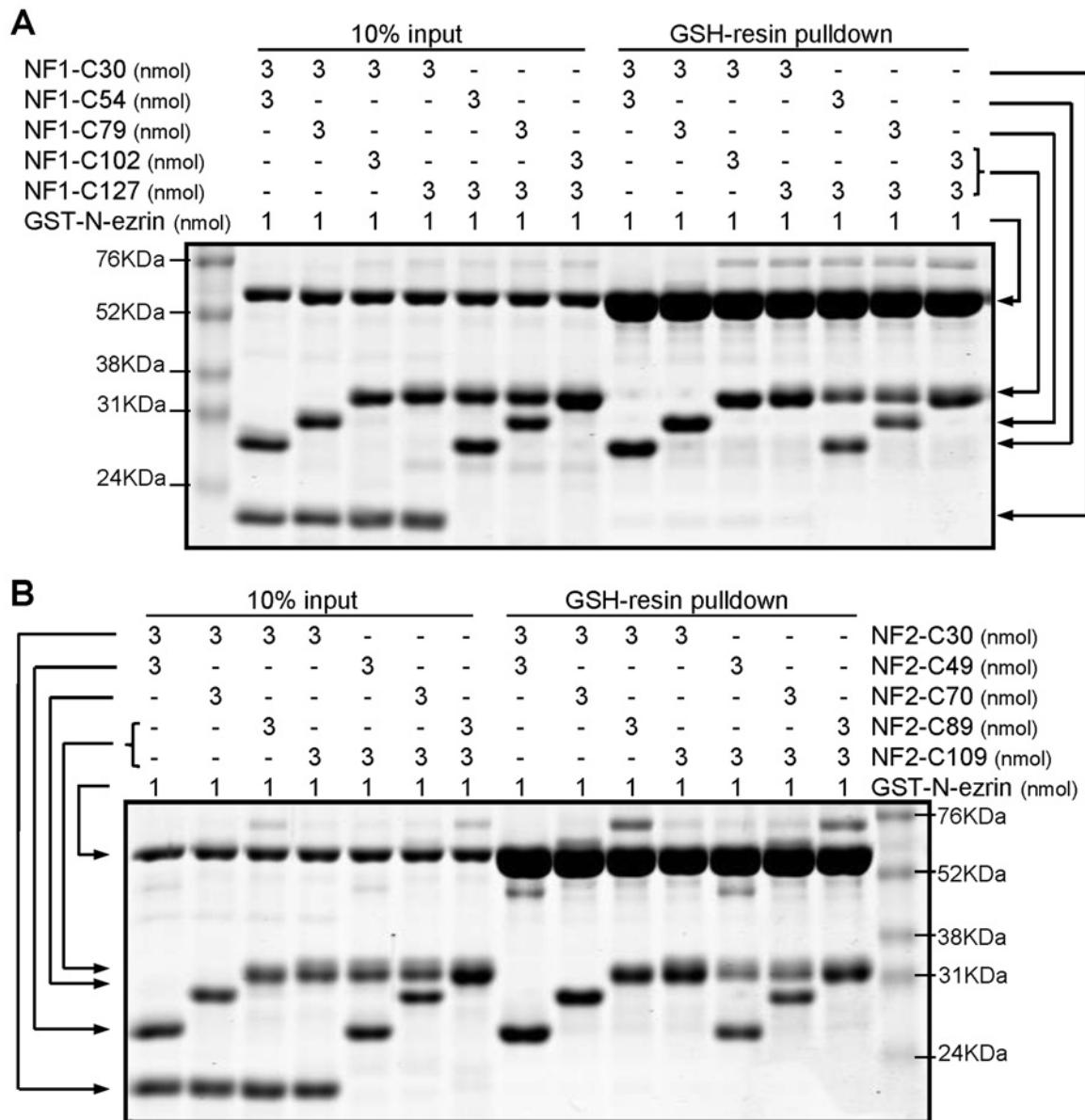
Figure 5   The essential non-conserved sequences required to enhance ezrin binding, are limited to 24 and 19 amino acid residues for NHERF1 and NHERF2 respectively

(**A**) GST–N–ezrin protein was mixed with NHERF1–C54, C79 or C102 in the presence of NHERF1–C30 or C127 as indicated for pull-downs. (**B**) GST-N–ezrin protein was mixed with NHERF2–C49, C70 or C89 in the presence of NHERF2–C30 or C109 as indicated for pull-downs. Both samples were analysed by Coomassie Blue staining. Experiments were repeated three times and one representative result is shown.

NHERF2–C109 (Figure 8C). NHERF2–C49 S303D, T305A and T305E could not compete with NHERF2-C109 (Figure 8C) and instead showed similar ezrin-binding capability to NHERF2–C30 (Figure 8B).

The effect of phosphomimetic mutations on ezrin-binding was further examined in full-length NHERF2 protein. FLAG–NHERF2 WT or mutants were transiently expressed in HEK-293A cells and cell lysate preparations were used for pull-down assays using purified GST-N–ezrin. Pull-down of the NHERF2–S303A mutant was similar to NHERF2–WT; whereas all the other single or double mutants showed less ezrin binding (Figure 9A). These results suggest that the interaction between NHERF2 and

ezrin is weakened by the phosphorylation of Ser[303] and probably also by phosphorylation of Thr[305]. However, caution has to be taken in interpreting the Thr[305] data because phosphor-mimicking and phosphor-deficient mutations of Thr[305] showed similar effects. This will be discussed later.

The ezrin-binding ability of full-length NHERF2–WT, S303A and S303D was investigated by co-IP. FLAG–NHERF2–WT, S303A and S303D transiently expressed in HEK-293A cells were precipitated with anti-FLAG conjugated beads. The co-IP of both ezrin and P-ezrin (phosphorylated ezrin) with the S303D mutant was reduced compared with co-IP of ezrin/P-ezrin with FLAG–NHERF2–WT (Figure 9B).
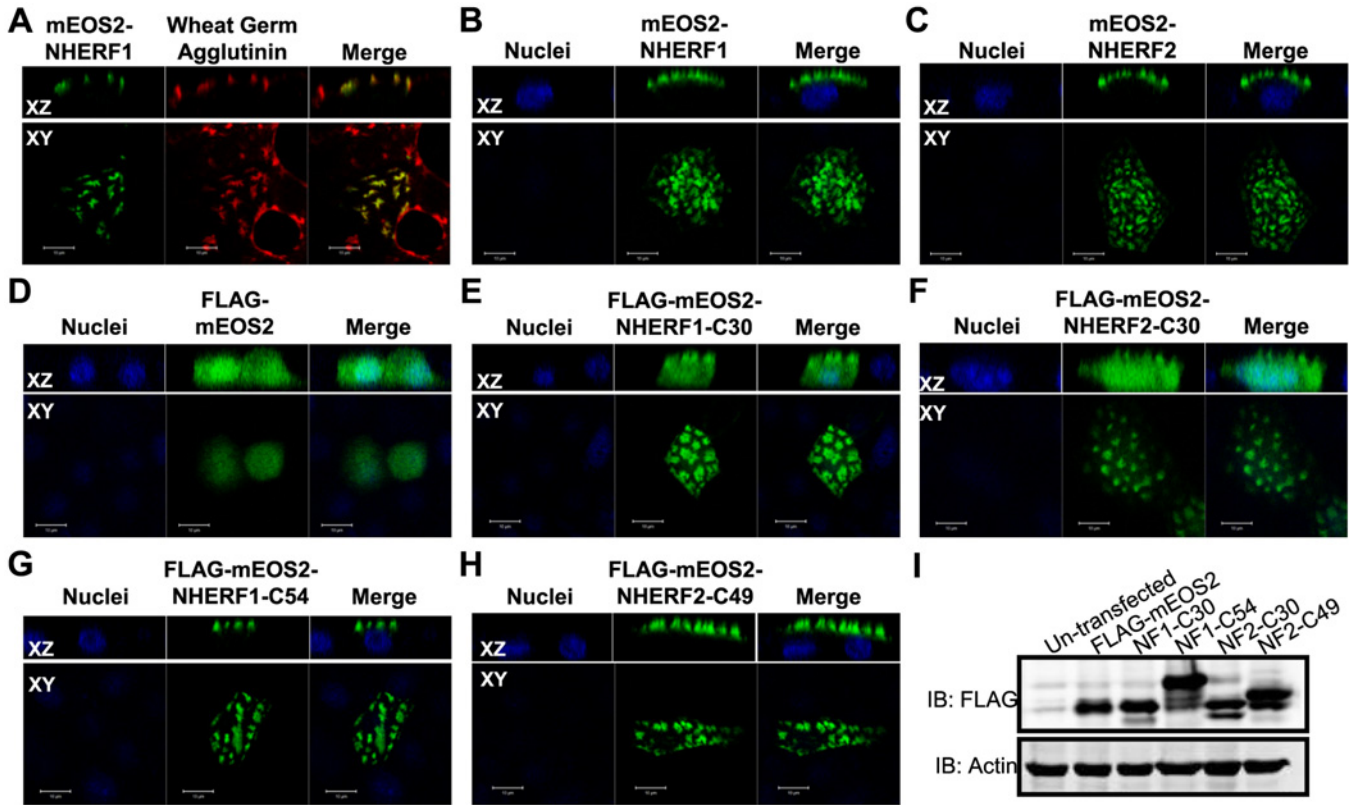
Figure 6   The EBRS of NHERF1/2 helps EBD to properly localize to the apical surface in polarized OK cells

(**A**) The primary apical distribution of transiently transfected mEOS2–NHERF1 co-localized with apical surface marker WGA in OK cells. Bottom, XY confocal images were taken at the apical surface of OK cells; Top, XZ images are slices of Z-section. Bar = 10 μm. (**B**–**H**) OK cells were transiently transfected with pmEOS2–NHERFs as indicated. Confocal imaging was performed with live cells after the nuclei were stained with Hoechst 33342. (**I**) FLAG–mEOS2 fused different NHERF1/2 C-termini proteins showed similar expression levels when transiently transfected into OK cells. Experiments were repeated three times and one representative result is shown.
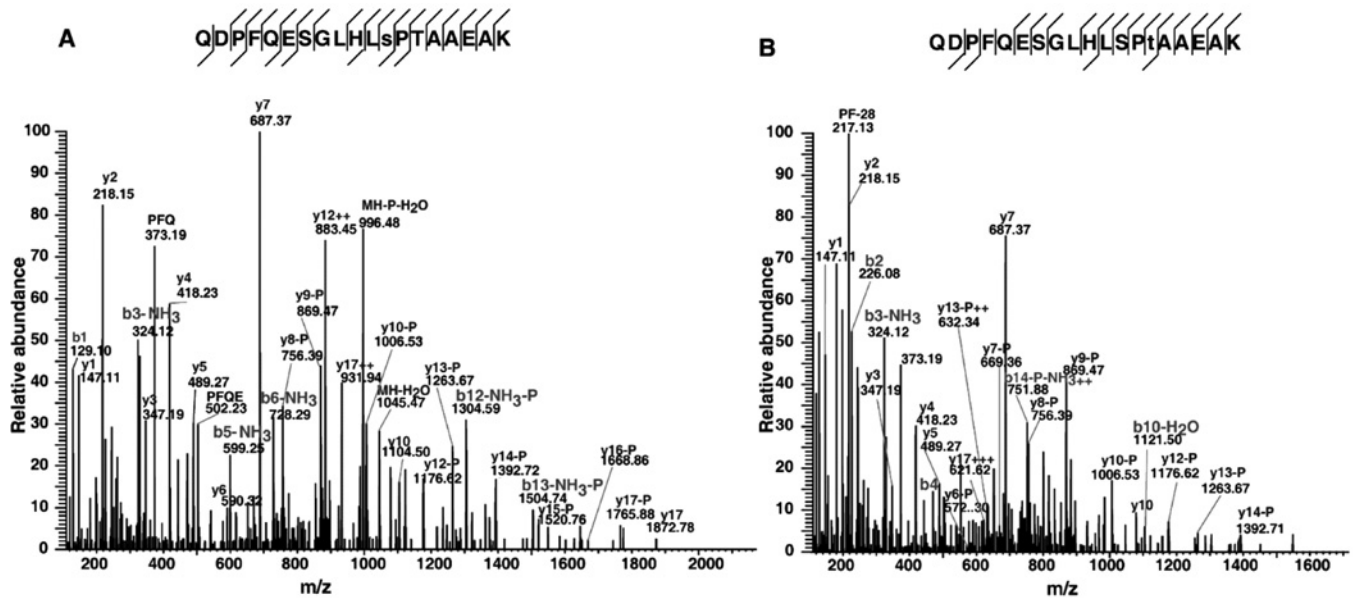

Figure 7   Identification of NHERF2 phosphorylation sites Ser303 and Thr305 by LC–MS/MS analysis of FLAG–NHERF2 IP sample

NHERF2 sample was immunoprecipitated from Caco-2/Bbe cells and proteolysed for LC–MS/MS analysis. Two phosphorylation sites were identified within the EBRS of NHERF2. MS/MS spectrum (**A**) shows the phosphorylation at Ser303. Presence of b12 and y8 ions with neutral loss phosphate indicate phosphorylation at Ser303 and in (**B**) presence of b14, y6 ions with the neutral loss phosphate indicate phosphorylation at Thr305 respectively. Phosphorylation analysis using MS was repeated in four separate experiments. Maximum Mascot score for Ser303 was 128 (range 42–128) and for Thr305 was 73 (range 43–73).
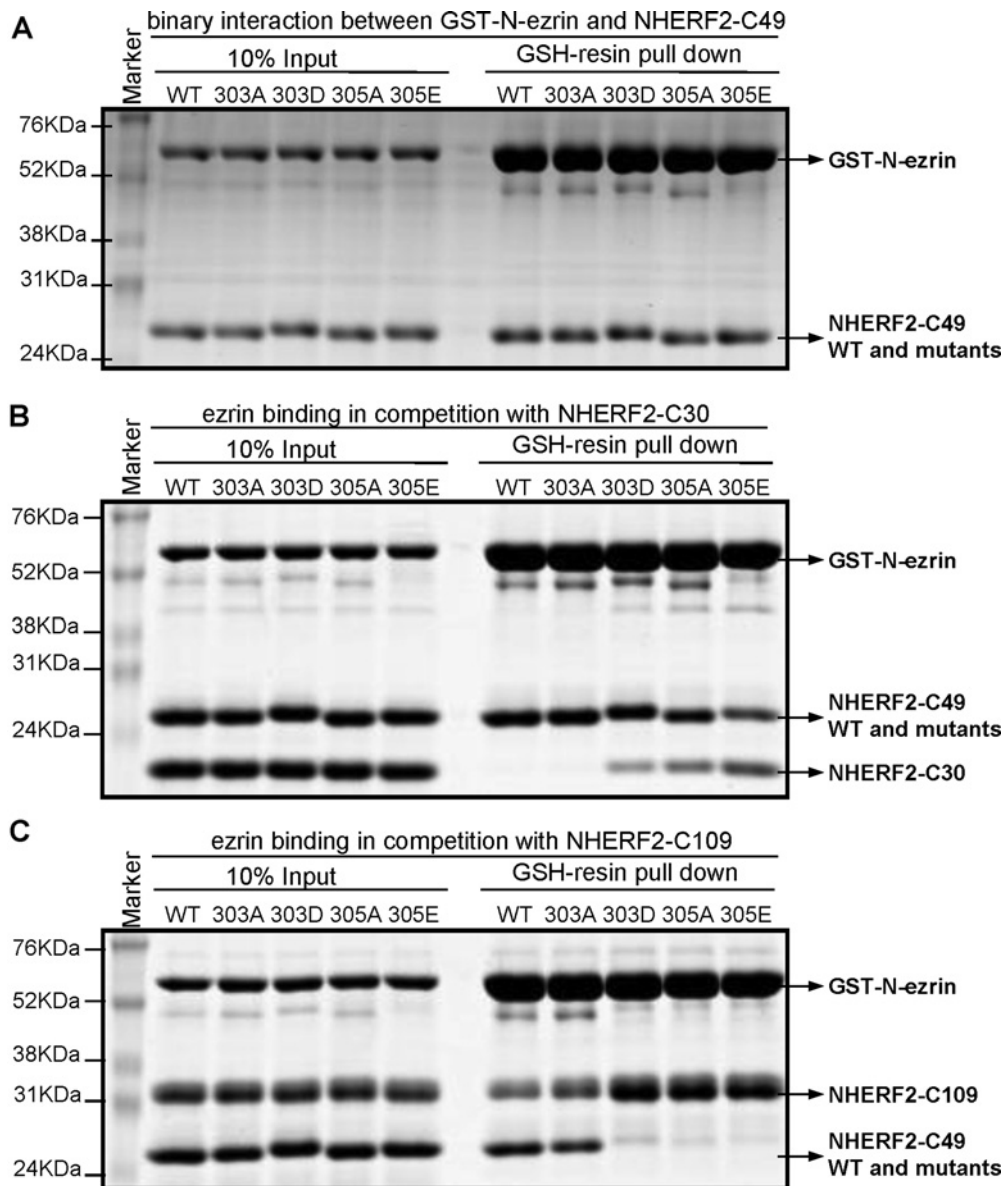
Figure 8   Ser[303] phosphomimetic mutant of NHERF2 has weaker interaction with ezrin

In the absence (**A**) or presence of 3 nmol of NHERF2–C30 (**B**) or NHERF2–C109 (**C**), 1 nmol of GST–N–ezrin protein was mixed with 3 nmol of individual NHERF2–C49, NHERF2–C49–S303A, S303D, T305A or T305E mutants and then subjected to pull-down. All samples were analysed by Coomassie Blue staining. Experiments were repeated three times and one representative result is shown.

Phosphorylation of Ser[303] dislocates NHERF2 from the apical surface to the cytosol and increases the microvillar mobility rate of NHERF2

The functional relevance of the Ser[303] phosphorylation was further studied by examining the protein localization in live OK cells. WT NHERF2 and NHERF2–S303A were both primarily distributed to the apical microvillar clusters, whereas NHERF2–S303D was localized in both the microvilli and the cytosol (Figure 10A). The similar abnormal cellular distribution of NHERF2–S303D and NHERF2–C30 (Figure 6) suggests that Ser[303] phosphorylation abolishes the function of NHERF2 EBRS.

FRAP was performed to study how much tighter these NHERF2 mutants are anchored in the microvilli. Consistent with our previous study, NHERF2 has a relatively slower microvillar mobility rate than NHERF1 [12]. NHERF2–S303A behaved

similarly to WT NHERF2. However, NHERF2–S303D had a faster mobility rate compared with both WT NHERF2 and NHERF1 (Figure 10B). This indicates that NHERF2–S303D is anchored more loosely in the microvilli than WT NHERF2 even though it can be distributed to the microvilli.

Functional significance of phosphorylation of NHERF2–Ser[303]

The functional significance of phosphorylation of NHERF2–Ser[303] was examined by exposing OK cells to dexamethasone for 4 h. Dexamethasone is known to stimulate NHE3 by an acute NHERF2-dependent effect that does not involve stimulation of transcription of NHE3 [43]. OK cells do not express detectable endogenous NHERF2 [43]. As shown in Figure 11, dexamethasone exposure stimulated NHE3 similarly in the
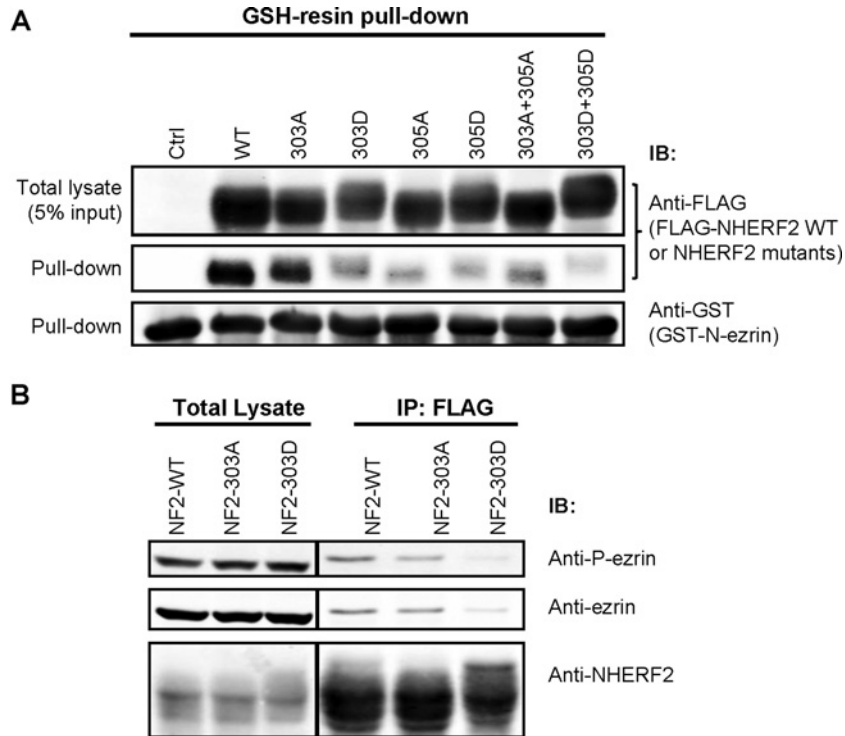
Figure 9   Binding of NHERF2 to ezrin is modulated by phosphorylation at Ser[303]

(**A**) Pull down was performed by mixing 3 μg of purified GST–N–ezrin and 1.5 mg cell lysate prepared from HEK-293A cells transiently transfected with FLAG–NHERF2–WT or mutants (S303A, S303D, T305A, T305D, S303A/T305A, S303D/T305D). The non-transfected HEK293 cell was used as a negative control (Ctrl). Samples were analysed by Western blot with antibodies against FLAG and GST. (**B**) HEK-293A cells transiently transfected with FLAG–NHERF2–WT or S303A or S303D mutant, were immunoprecipitated with anti-FLAG M2 magnetic beads. IP/co-IP samples were analysed by Western blot with antibodies against FLAG, ezrin and P-ezrin.
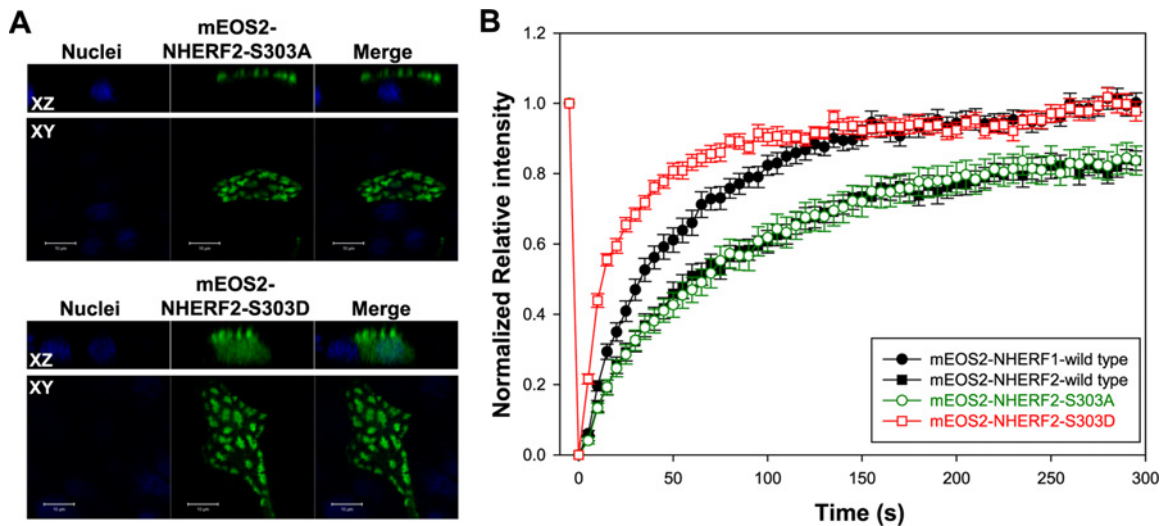

Figure 10   Ser[303] phosphomimetic mutation induces the cytosolic distribution of NHERF2 in OK cells and increases its microvillar mobility rate

(**A**) Confocal imaging was performed with live OK cells transiently transfected with pmEOS2–NHERF2–S303A and S303D after the nuclei were stained with Hoechst 33342. (**B**) FRAP studies were performed with OK cells transiently transfected with pmEOS2-NHERFs. Fluorescence recovery ratio was normalized by total quenched fluorescence intensity, averaged from 16 cells, compared among mEOS2–NHERF1 (●), mEOS2–NHERF2 (■), mEOS2–NHERF2–S303A (○) and mEOS2–NHERF2–S303D (□). Error bars represent S.E.M. The data points of mEOS2–NHERF1 and of mEOS2–NHERF2–S303D after 15 s are significantly different from that of the other three traces ($P < 0.05$).

presence of exogenous WT NHERF2 and NHERF2–S303A but not when NHERF2–S303D was expressed. NHE3–S303D basal activity was increased compared with WT NHE3 (Figure 11). These results are consistent with the dexamethasone effect requiring NHERF2–ezrin binding to mediate the assembly of a NHE3 signalling complex on the apical membrane [43] and demonstrate functional significance of phosphorylation of NHERF2–Ser[303].

DISCUSSION

With the effort to answer why NHERF2 is more fixed in the microvilli with a slower mobility rate in comparison with NHERF1, the current study identified an EBRS located in the non-conserved regions immediately upstream of the EBD in both NHERF1 and NHERF2. The EBRS not only biochemically enhances the interaction between EBD and ezrin, but it also is functionally necessary for the exclusive apical localization of NHERF proteins. Also importantly, phosphorylation of NHERF2 EBRS serves as a regulatory mechanism for ezrin binding. Phosphorylation of Ser[303] in NHERF2 EBRS decreases the strength of interaction between NHERF2 and ezrin as well as induces the redistribution of NHERF2 from apical microvilli to the cytosol.

Multiple scaffolding proteins have been recognized as being highly mobile, although they are specifically localized to stable cellular structures such as microvilli, tight junctions and neuronal synapses [5,24–27]. The mobility of these scaffolding proteins was determined by the on and off rate of their dynamic interaction with their binding partners inside of cellular structures. Changes in the interaction between scaffolding proteins and their partners also cause the changes in their mobility. For example, ezrin mobility is mainly determined by its interaction with PIP2, F-actin or their synergistic effect and is regulated by phosphorylation [24,44].

To search for the critical partners determining the slower microvillar mobility of NHERF2 compared with NHERF1, we have defined the critical domains or sequences that distinguish NHERF2 from NHERF1 [12]. The contribution of PDZ domains to stabilizing NHERF2 in the microvilli has been ruled out previously by study of PDZ domain mutants in both OK and JEG-3 cells [12,35]. Concerning NHERF1, interaction between PDZ domains and their ligands increased NHERF1 mobility in JEG-3 [35], but had no effect on NHERF1 mobility in OK cells [12]. Swapping only the EBD between NHERF1 and NHERF2 did not switch their mobility rates, suggesting EBD alone is not sufficient. Instead, the combination of EBD and its upstream non-conserved region distinguished NHERF2 from NHERF1 in a series of properties including NHERF2's higher detergent insolubility, larger size of cytoskeleton complexes and a slower mobility rate in OK cell microvilli [12]. This was later confirmed in human placental choriocarcinoma JEG-3 cells [23].

The unexplained role of the non-conserved region upstream of EBD is now resolved by the discovery of EBRS within this region. In both NHERF1 and NHERF2, EBRSs enhance the interaction between EBDs and ezrin. Although EBDs of NHERF1 and NHERF2 are necessary for the interaction with ezrin [14,15,29], they are not sufficient to mimic the full-length NHERF1/2 proteins based on three observations. First, full-length NHERF2 has higher affinity for ezrin than full-length NHERF1, whereas NHERF2–EBD has lower affinity for ezrin than NHERF1–EBD. Second, EBDs are not sufficient to compete with full-length NHERF1/2 proteins in ezrin binding. Third, EBDs are not sufficient to be exclusively localized to the apical surface. However, in all three cases, the combination of EBRS and EBD is able to fully
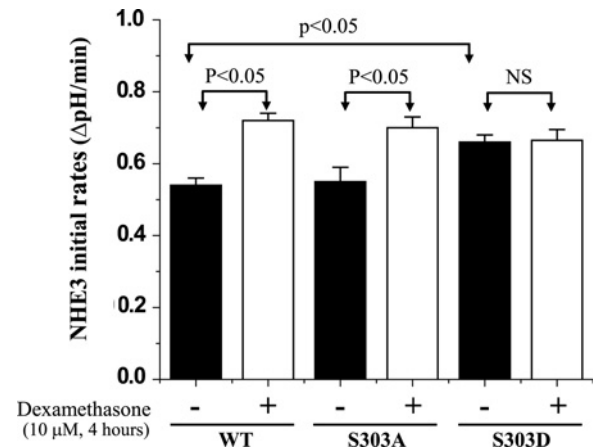

Figure 11   Expression of the NHERF2–S303D mutant in OK cells does not allow the NHERF2-dependent dexamethasone stimulation of NHE3 activity

NHE3 activity was measured in OK cells transfected with NHERF2–WT, S303A and S303D and exposed to dexamethasone, 10 μM, 4 h. Dexamethasone stimulated NHE3 activity equally in cells transfected with WT and NHERF2–S303A but not in cells transfected with NHERF2–S303D. Results are means $\pm$ S.E.M. of four separate experiments. *P*-values compare dexamethasone stimulation of NHE3 in WT NHERF2 expressing cells with that in cells expressing NHERF2–S303A and S303D (paired *t* tests).

mimic the full-length NHERF1/2. Thus, EBRSs co-operate with EBDs to determine the overall affinities of NHERF1/2 for ezrin. In addition, the ezrin-binding strengths of all NHERF1/2 C-termini are correlated with the extent of their apical localization, suggesting that NHERF1/2 proteins are most probably anchored in the microvilli through their interaction with ezrin.

Identification of EBRS revealed another important function for the non-conserved linkers in NHERF1/2. In NHERF1 and NHERF2, the linker between the two PDZ domains and the linker between the PDZ2 and EBD are non-conserved. Several studies have shown these linkers also play important roles. In NHERF1, mutation of L110V in the linker between its two PDZ domains causes hyper-responsiveness of renal parathyroid hormone and impaired renal phosphate re-absorption [45]. In NHERF1, the adjacent sequences downstream of the classically defined PDZ2 (which are upstream and distinct from the EBRS) have been proposed to stabilize the structure of PDZ2 and affect its ligand binding [46]. In NHERF2, the non-conserved linker between PDZ2 and EBD is required for the interaction with both NHE3 [15] and α-actinin-4 [47]. Although the 3D structures of the NHERF1/NHERF2 PDZ and EBD domains have been resolved, the structural information of the non-conserved linkers is very limited. How these non-conserved linkers affect the function of NHERF1/2 is still unknown and awaits insights from studies that provide structural information.

The important role of EBRS in ezrin binding is also corroborated by the fact that phosphorylation of Ser[303] in EBRS decreased the interaction between NHERF2 and ezrin and consequently dislocated NHERF2 from the apical surface to the cytosol. A similar phenomenon has been shown in canine NHERF1 in that double phosphorylation of S347/S348 by PKC led to the dissociation of NHERF1 from ezrin and redistribution to the cytosol [37]. Canine NHERF1 S347/S348 residues correspond to S339/S340 in human NHERF1. These two serine residues are located within the EBD of NHERF1 and are conserved across species (Figure 1C). Although EBD domain of NHERF1 and NHERF2 are very similar, these two serine residues are not present in NHERF2 and the comparable residues in NHERF2 are valine and aspartic acid. In contrast, Ser[303] is conserved across species

in NHERF2 but not in NHERF1, corresponding to asparagine in human NHERF1 (Figure 1C).

In our study, both NHERF2 Ser^{303} and Thr^{305} were found to be phosphorylated. Emphasis in attributing a role of NHERF2 Ser^{303} phosphorylation is based on the difference in the effects of the aspartic acid compared with alanine mutations consistent with there being an effect via changes in phosphorylation. The role of Thr^{305} phosphorylation in ezrin binding is not clear since the alanine, aspartic acid and glutamic acid mutations similarly reduced ezrin binding. This does not exclude that phosphorylation of Thr^{305} regulates the interaction between NHERF2 and ezrin, but instead indicates that the threonine hydroxy group may be involved in the formation of a critical hydrogen bond with a neighbouring residue and leaves the possibility that any substitutions in the amino acid at Thr^{305} could affect ezrin binding. NHERF2 Thr^{305} is also conserved across species and corresponds to a conserved serine residue in NHERF1, which has not been reported to be phosphorylated.

The interaction between EBDs of NHERF1/2 and FERM domain of ERM proteins has been studied by co-crystallization [29]. Though the carboxy 28 residues were used for the study, only the last 13 residues of EBDs form an amphipathic α-helix and are involved in direct interaction with the FERM domain. Other residues including S339/S340 in human NHERF1 are either disordered or not resolved in the structure [29]. Further structural analysis is required to understand the function of the EBRS and the mechanism by which phosphorylation of S339/S340 in NHERF1 and of Ser^{303} in NHERF2 affects ezrin binding.

These are the initial functional studies demonstrating a role for phosphorylation of NHERF2 in ligand binding and determining its localization in the apical domain of epithelial cells. NHERF2 binds apical proteins of multiple classes, including channels and GPCRs in addition to transporters, generally stabilizing them to the cell cortex [3,4,13,48]. This often occurs via indirect linking to cytoskeleton through ezrin binding [14,15]. Identification of the kinases involved in phosphorylation of NHERF2 Ser^{303} and perhaps Thr^{305} and the circumstances that alter this phosphorylation is likely to reveal more about the function of the NHERF2 which until now has largely been portrayed as a static scaffold. Importantly, now that NHERF2 has been shown to be phosphorylated, the role of these phosphorylations in multiple NHERF2 functions needs to be defined.

AUTHOR CONTRIBUTION

Jianbo Yang, Rafiquel Sarker, Varsha Singh, Xuhang Li, Ming Tse and Mark Donowitz participated in research design. Jianbo Yang, Rafiquel Sarker, Varsha Singh, Jianyi Yin, Prateeti Sarker, Raghothama Chaerkady and Tian-E Chen performed experiments. Data analysis and interpretation was done by Jianbo Yang, Rafiquel Sarker, Raghothama Chaerkady and Mark Donowitz. Jianbo Yang, Rafiquel Sarker and Mark Donowitz wrote the manuscript. Jianbo Yang conceived and developed experiments for Figures 1–6, 8 and 10. Rafiquel Sarker conceived and developed experiments for Figures 7, 9 and 11.

REFERENCES

1 Lange, K. (2011) Fundamental role of microvilli in the main functions of differentiated cells: Outline of an universal regulating and signaling system at the cell periphery. J. Cell. Physiol. **226**, 896–927 CrossRef PubMed

2 Fehon, R.G., McClatchey, A.I. and Bretscher, A. (2010) Organizing the cell cortex: the role of ERM proteins. Nat. Rev. Mol. Cell Biol. **11**, 276–287 CrossRef PubMed

3 Donowitz, M., Cha, B., Zachos, N.C., Brett, C.L., Sharma, A., Tse, C.M. and Li, X. (2005) NHERF family and NHE3 regulation. J. Physiol. **567**, 3–11 CrossRef PubMed

4 Romero, G., von Zastrow, M. and Friedman, P.A. (2011) Role of PDZ proteins in regulating trafficking, signaling, and function of GPCRs: means, motif, and opportunity. Adv. Pharmacol. **62**, 279–314 CrossRef PubMed

5 Garbett, D. and Bretscher, A. (2014) The surprising dynamics of scaffolding proteins. Mol. Biol. Cell. **25**, 2315–2319 CrossRef PubMed

6 Niggli, V., Andreoli, C., Roy, C. and Mangeat, P. (1995) Identification of a phosphatidylinositol-4,5-bisphosphate-binding domain in the N-terminal region of ezrin. FEBS Lett **376**, 172–176 CrossRef PubMed

7 Cha, B., Tse, M., Yun, C., Kovbasnjuk, O., Mohan, S., Hubbard, A., Arpin, M. and Donowitz, M. (2006) The NHE3 juxtamembrane cytoplasmic domain directly binds ezrin: dual role in NHE3 trafficking and mobility in the brush border. Mol. Biol. Cell. **17**, 2661–2673 CrossRef PubMed

8 Denker, S.P., Huang, D.C., Orlowski, J., Furthmayr, H. and Barber, D.L. (2000) Direct binding of the Na–H exchanger NHE1 to ERM proteins regulates the cortical cytoskeleton and cell shape independently of H(+) translocation. Mol. Cell. **6**, 1425–1436 CrossRef PubMed

9 Viswanatha, R., Wayt, J., Ohouo, P.Y., Smolka, M.B. and Bretscher, A. (2013) Interactome analysis reveals ezrin can adopt multiple conformational states. J. Biol. Chem. **288**, 35437–35451 CrossRef PubMed

10 Gary, R. and Bretscher, A. (1995) Ezrin self-association involves binding of an N-terminal domain to a normally masked C-terminal domain that includes the F-actin binding site. Mol. Biol. Cell. **6**, 1061–1075 CrossRef PubMed

11 Turunen, O., Wahlstrom, T. and Vaheri, A. (1994) Ezrin has a COOH-terminal actin-binding site that is conserved in the ezrin protein family. J. Cell Biol. **126**, 1445–1453 CrossRef PubMed

12 Yang, J., Singh, V., Cha, B., Chen, T.E., Sarker, R., Murtazina, R., Jin, S., Zachos, N.C., Patterson, G.H., Tse, C.M. et al. (2013) NHERF2 protein mobility rate is determined by a unique C-terminal domain that is also necessary for its regulation of NHE3 protein in OK cells. J. Biol. Chem. **288**, 16960–16974 CrossRef PubMed

13 Seidler, U., Singh, A.K., Cinar, A., Chen, M., Hillesheim, J., Hogema, B. and Riederer, B. (2009) The role of the NHERF family of PDZ scaffolding proteins in the regulation of salt and water transport. Ann. N.Y. Acad. Sci. **1165**, 249–260 CrossRef PubMed

14 Reczek, D. and Bretscher, A. (1998) The carboxyl-terminal region of EBP50 binds to a site in the amino-terminal domain of ezrin that is masked in the dormant molecule. J. Biol. Chem. **273**, 18452–18458 CrossRef PubMed

15 Yun, C.H., Lamprecht, G., Forster, D.V. and Sidor, A. (1998) NHE3 kinase A regulatory protein E3KARP binds the epithelial brush border Na+/H+ exchanger NHE3 and the cytoskeletal protein ezrin. J. Biol. Chem. **273**, 25856–25863 CrossRef PubMed

16 Cha, B., Kenworthy, A., Murtazina, R. and Donowitz, M. (2004) The lateral mobility of NHE3 on the apical membrane of renal epithelial OK cells is limited by the PDZ domain proteins NHERF1/2, but is dependent on an intact actin cytoskeleton as determined by FRAP. J. Cell Sci. **117**, 3353–3365 CrossRef PubMed

17 Singh, V., Lin, R., Yang, J., Cha, B., Sarker, R., Tse, C.M. and Donowitz, M. (2014) AKT and GSK-3 are necessary for direct ezrin binding to NHE3 as part of a C-terminal stimulatory complex: role of a novel Ser-rich NHE3 C-terminal motif in NHE3 activity and trafficking. J. Biol. Chem. **289**, 5449–5461 CrossRef PubMed

18 Schultheis, P.J., Clarke, L.L., Meneton, P., Miller, M.L., Soleimani, M., Gawenis, L.R., Riddle, T.M., Duffy, J.J., Doetschman, T., Wang, T. et al. (1998) Renal and intestinal absorptive defects in mice lacking the NHE3 Na+/H+ exchanger. Nat. Genet. **19**, 282–285 CrossRef PubMed

19 Singh, V., Yang, J., Chen, T.E., Zachos, N.C., Kovbasnjuk, O., Verkman, A.S. and Donowitz, M. (2014) Translating molecular physiology of intestinal transport into pharmacologic treatment of diarrhea: stimulation of Na+ absorption. Clin. Gastroenterol. Hepatol. **12**, 27–31 CrossRef PubMed

20 Chen, T., Hubbard, A., Murtazina, R., Price, J., Yang, J., Cha, B., Sarker, R. and Donowitz, M. (2014) Myosin VI mediates the movement of NHE3 down the microvillus in intestinal epithelial cells. J. Cell Sci. **127**, 3535–3545 CrossRef PubMed

21 Sarker, R., Valkhoff, V.E., Zachos, N.C., Lin, R., Cha, B., Chen, T.E., Guggino, S., Zizak, M., de Jonge, H., Hogema, B. and Donowitz, M. (2011) NHERF1 and NHERF2 are necessary for multiple but usually separate aspects of basal and acute regulation of NHE3 activity. Am. J. Physiol. Cell. Physiol. **300**, C771–C782 CrossRef PubMed

22 Zhu, X., Cha, B., Zachos, N.C., Sarker, R., Chakraborty, M., Chen, T.E., Kovbasnjuk, O. and Donowitz, M. (2011) Elevated calcium acutely regulates dynamic interactions of NHERF2 and NHE3 in OK cell Microvilli. J. Biol. Chem. **286**, 34486–34496 CrossRef PubMed

23 Garbett, D., Sauvanet, C., Viswanatha, R. and Bretscher, A. (2013) The tails of apical scaffolding proteins EBP50 and E3KARP regulate their localization and dynamics. Mol. Biol. Cell. **24**, 3381–3392 CrossRef PubMed

24 Coscoy, S., Waharte, F., Gautreau, A., Martin, M., Louvard, D., Mangeat, P., Arpin, M. and Amblard, F. (2002) Molecular analysis of microscopic ezrin dynamics by two-photon FRAP. Proc. Natl. Acad. Sci. U.S.A. **99**, 12813–12818 CrossRef PubMed

25 Waharte, F., Brown, C.M., Coscoy, S., Coudrier, E. and Amblard, F. (2005) A two-photon FRAP analysis of the cytoskeleton dynamics in the microvilli of intestinal cells. Biophys. J. **88**, 1467–1478 CrossRef PubMed

26 Tyska, M.J. and Mooseker, M.S. (2002) MYO1A (brush border myosin I) dynamics in the brush border of LLC-PK1-CL4 cells. Biophys. J. **82**, 1869–1883 CrossRef PubMed

27 Zheng, C.Y., Petralia, R.S., Wang, Y.X., Kachar, B. and Wenthold, R.J. (2010) SAP102 is a highly mobile MAGUK in spines. J. Neurosci. **30**, 4757–4766 CrossRef PubMed

28 Morales, F.C., Takahashi, Y., Momin, S., Adams, H., Chen, X. and Georgescu, M.M. (2007) NHERF1/EBP50 head-to-tail intramolecular interaction masks association with PDZ domain ligands. Mol. Cell. Biol. **27**, 2527–2537 CrossRef PubMed

29 Terawaki, S., Maesaki, R. and Hakoshima, T. (2006) Structural basis for NHERF recognition by ERM proteins. Structure **14**, 777–789 CrossRef PubMed

30 Finnerty, C.M., Chambers, D., Ingraffea, J., Faber, H.R., Karplus, P.A. and Bretscher, A. (2004) The EBP50-moesin interaction involves a binding site regulated by direct masking on the FERM domain. J. Cell Sci. **117**, 1547–1552 CrossRef PubMed

31 Boratko, A. and Csortos, C. (2013) NHERF2 is crucial in ERM phosphorylation in pulmonary endothelial cells. Cell Commun. Signal. **11**, 99 CrossRef PubMed

32 Algrain, M., Turunen, O., Vaheri, A., Louvard, D. and Arpin, M. (1993) Ezrin contains cytoskeleton and membrane binding domains accounting for its proposed role as a membrane-cytoskeletal linker. J. Cell Biol. **120**, 129–139 CrossRef PubMed

33 Yang, J., Singh, V., Chen, T.E., Sarker, R., Xiong, L., Cha, B., Jin, S., Li, X., Tse, C.M., Zachos, N.C. and Donowitz, M. (2014) NHERF2/NHERF3 protein heterodimerization and macrocomplex formation are required for the inhibition of nhe3 activity by carbachol. J. Biol. Chem. **289**, 20039–20053 CrossRef PubMed

34 Wisniewski, J.R., Zougman, A., Nagaraj, N. and Mann, M. (2009) Universal sample preparation method for proteome analysis. Nat. Methods **6**, 359–362 CrossRef PubMed

35 Garbett, D. and Bretscher, A. (2012) PDZ interactions regulate rapid turnover of the scaffolding protein EBP50 in microvilli. J. Cell Biol. **198**, 195–203 CrossRef PubMed

36 Cole, J.A., Forte, L.R., Krause, W.J. and Thorne, P.K. (1989) Clonal sublines that are morphologically and functionally distinct from parental OK cells. Am. J. Physiol. **256**, F672–F679 PubMed

37 Chen, J.Y., Lin, Y.Y. and Jou, T.S. (2012) Phosphorylation of EBP50 negatively regulates beta-PIX-dependent Rac1 activity in anoikis. Cell Death Differ **19**, 1027–1037 CrossRef PubMed

38 Hornbeck, P.V., Kornhauser, J.M., Tkachev, S., Zhang, B., Skrzypek, E., Murray, B., Latham, V. and Sullivan, M. (2012) PhosphoSitePlus: a comprehensive resource for investigating the structure and function of experimentally determined post-translational modifications in man and mouse. Nucleic Acids Res **40**, D261–D270 CrossRef PubMed

39 Wisniewski, J.R., Nagaraj, N., Zougman, A., Gnad, F. and Mann, M. (2010) Brain phosphoproteome obtained by a FASP-based method reveals plasma membrane protein topology. J. Proteome Res. **9**, 3280–3289 CrossRef PubMed

40 Lundby, A., Secher, A., Lage, K., Nordsborg, N.B., Dmytriyev, A., Lundby, C. and Olsen, J.V. (2012) Quantitative maps of protein phosphorylation sites across 14 different rat organs and tissues. Nat. Commun. **3**, 876 CrossRef PubMed

41 Sharma, K., D'Souza, R.C., Tyanova, S., Schaab, C., Wisniewski, J.R., Cox, J. and Mann, M. (2014) Ultradeep human phosphoproteome reveals a distinct regulatory nature of Tyr and Ser/Thr-based signaling. Cell Rep **8**, 1583–1594 CrossRef PubMed

42 Zhou, H., Di Palma, S., Preisinger, C., Peng, M., Polat, A.N., Heck, A.J. and Mohammed, S. (2013) Toward a comprehensive characterization of a human cancer cell phosphoproteome. J. Proteome Res. **12**, 260–271 CrossRef PubMed

43 Yun, C.C., Chen, Y. and Lang, F. (2002) Glucocorticoid activation of Na$(+)$/H$(+)$ exchanger isoform 3 revisited. The roles of SGK1 and NHERF2. J. Biol. Chem. **277**, 7676–7683 CrossRef PubMed

44 Fritzsche, M., Thorogate, R. and Charras, G. (2014) Quantitative analysis of ezrin turnover dynamics in the actin cortex. Biophys. J. **106**, 343–353 CrossRef PubMed

45 Karim, Z., Gerard, B., Bakouh, N., Alili, R., Leroy, C., Beck, L., Silve, C., Planelles, G., Urena-Torres, P., Grandchamp, B. et al. (2008) NHERF1 mutations and responsiveness of renal parathyroid hormone. N. Engl. J. Med. **359**, 1128–1135 CrossRef PubMed

46 Bhattacharya, S., Dai, Z., Li, J., Baxter, S., Callaway, D.J., Cowburn, D. and Bu, Z. (2010) A conformational switch in the scaffolding protein NHERF1 controls autoinhibition and complex formation. J. Biol. Chem. **285**, 9981–9994 CrossRef PubMed

47 Kim, J.H., Lee-Kwon, W., Park, J.B., Ryu, S.H., Yun, C.H. and Donowitz, M. (2002) Ca$(2+)$-dependent inhibition of Na$+$/H$+$ exchanger 3 (NHE3) requires an NHE3-E3KARP-alpha-actinin-4 complex for oligomerization and endocytosis. J. Biol. Chem. **277**, 23714–23724 CrossRef PubMed

48 Wade, J.B., Liu, J., Coleman, R.A., Cunningham, R., Steplock, D.A., Lee-Kwon, W., Pallone, T.L., Shenolikar, S. and Weinman, E.J. (2003) Localization and interaction of NHERF isoforms in the renal proximal tubule of the mouse. Am. J. Physiol. Cell Physiol. **285**, C1494–C1503 CrossRef PubMed